Effective refractive index of the photonic crystal deduced from the oscillation model of the membrane

Ting-Hang Pei[1,*] and Yang-Tung Huang[2]

[1]*Microelectronics and Information Systems Research Center, National Chiao Tung University,
30010, Hsinchu, Taiwan, China*
[2]*Department of Electronics Engineering and Institute of Electronics, National Chiao Tung University,
1001 Ta-Hsueh Road, 30010, Hsinchu, Taiwan, China*
Corresponding author: thp3000.ee88g@nctu.edu.tw

The oscillation model of the circular membrane is used to calculate the effective refractive index of the two-dimensional triangular photonic crystal at normal incidence within the second photonic band. Negatively effective refractive indices deduced from this model match those calculated by equifrequency surfaces very well. The result reveals that the field distribution has relation with the effective refractive index at certain frequency regions. Besides, the field distribution described by the Bessel function is more compact than the Fourier series expansion.   © 2012 Optical Society of America

OCIS codes: 050.5298, 120.5710, 260.2065, 350.4238.

1. INTRODUCTION

The photonic crystal (PhC) is formed with dielectric periodic structure, which has the photonic band structure (PBS) and exhibits new electromagnetic phenomena [1,2]. Two of them are the superprism effect [3] and negativelike refraction [4–11]. The former has been demonstrated experimentally by Kosaka *et al.* in 1998 [3]. They found that the refracted angle of a light beam in the PhC is very sensitive to the incident angle and wavelength. The basic explanation of the superprism effect is the anomalous dispersion characteristics of the PBS of the PhC. As we know, the propagation direction of light in the PhC is the same as the direction of the group velocity, which is determined by and parallel to the equifrequency surface (EFS) [11]. Given the incident wave vector with a corresponding frequency and an incident angle, the refracted wave vector as well as the refracted angle can be determined.

Recently, negativelike refractions in PhCs have attracted much attention [4–11]. They discussed optical properties of PhCs by considering the frequency-dependent permittivity $\varepsilon(\omega)$, permeability $\mu(\omega)$, and negative refractive index $n(\omega)$ defined as $-\sqrt{\varepsilon(\omega)\mu(\omega)}$. These often take place in higher photonic bands. In our previous works [13–15], we focused on the effective refractive index within the first photonic band only. The Bloch wave inside the PhC is very close to that in the effectively homogeneous medium so the replacement is very accurate. However, it is not true in the higher photonic bands because the compositions of the Bloch waves are more complicated. More and more nonignored Fourier terms enter into the Bloch waves and display anomalously optical properties. Even the effective refractive index can simply explain refractions in higher photonic bands; however, the field distribution is far away from this simple concept. Although the field distribution is very complicated, it is possible to extract some information about optical performances from the field distribution. For example, we can deduce the negatively effective refractive indices from the field distributions as we do in this paper. Traditionally, the effective refractive index is calculated from EFSs. The more are the Fourier series added, the more accurate effective refractive index we obtain. But it needs a lot of time to obtain the effective refractive index this way. If the equation of the effective refractive index for the higher photonic bands can be obtained, it benefits the applications of the PhC and also reduces the computation time explicitly.

In this paper, we extend attention to the part of the second photonic band of the two-dimensional (2D) triangular PhC, where the effective refractive index is negatively defined. By observing field distributions, the oscillation model of the circular membrane is proposed. The field distribution in the PhC is replaced with the amplitude of the circular membrane. Then we can deduce the negatively effective refractive index at normal incidence by this model.

2. 2D PHOTONIC CRYSTAL CASE

A. Photonic Band Structure and Equifrequency Surfaces

We consider a 2D PhC composed of a triangular array of air cylinders with dielectric constant $\varepsilon_b = 1.0$ laid on the x-y plane. These cylinders are embedded into a background medium of which the dielectric constant $\varepsilon_a = 1.0$ is 12.25. The lattice constant of the triangular array is a, and the radius r of air cylinders is $0.42a$ The PBS of this PhC is shown in Fig. 1(a), in which the bold curve denotes the second photonic bands. A total of 5041 plane waves are used in calculations and errors are below 0.5%. The same number of plane waves is also used to calculate EFSs from 0.345 to $0.365(c/a)$ as shown in Fig. 1(b). In order to investigate the field distribution in the PhC, the case of the Gaussian wave normally incident from air into a finite PhC is calculated by the finite-difference time-domain (FDTD) method [16]. The interface between air and the finite PhC is along the ΓK direction, and the
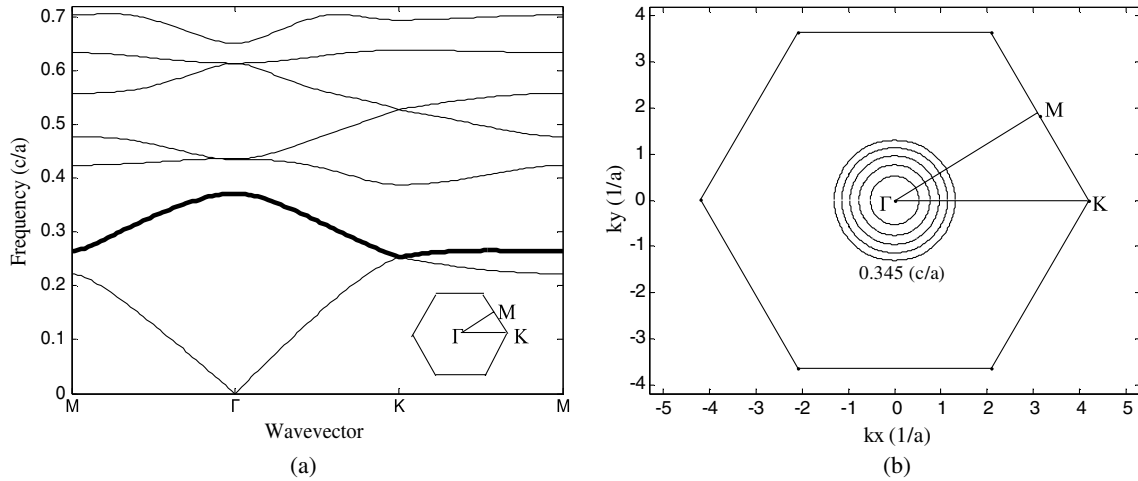
Fig. 1. (a) PBS of a 2D triangular photonic crystal with $\varepsilon_a = 12.25$, $\varepsilon_b = 1.0$, and $r = 0.42a$. The bold curve denotes second photonic band. (b) EFSs in the first Brillouin zone where frequencies are uniformly between 0.345 and 0.365(c/a) from the outermost curve to the innermost one.

propagation direction of the Gaussian wave is along the ΓM direction, where the ΓM and ΓK directions are parallel to x- and y-axes, respectively. Because the EFS shrinks as the frequency increases in this photonic band, the effective refractive indices are principally negative except for the bottom of this band.

B. Field Distribution in the Photonic Crystal

First, we investigate the field distributions in the PhC by utilizing the FDTD method. A TM-polarized (E-field is parallel to the cylinder) Gaussian wave of $0.36(c/a)$ is normally incident on the PhC, where c is the speed of light in vacuum. This frequency is close to the top of the second photonic band and its EFS as well as other frequencies are shown in Fig. 1(b). The innermost curve corresponds to $0.365(c/a)$, and the outmost one corresponds to $0.345(c/a)$. The frequency uniformly increases from the outmost to the innermost, where the interval is $0.005(c/a)$. After propagating enough distance in the PhC, the incident wave becomes the Bloch wave as shown in Fig. 2(a). The periodic length of the field or the Bloch wavelength λ_{Bloch} is about $10.4a$. Here the Bloch wavelength is found from the field distribution as shown in Fig. 2(a). It represents the period of the field distribution in the propagation direction and is $2\pi/k_{\mathrm{Bloch}}$, where k_{Bloch} is the Bloch wave vector. As seen from the E_z-field distribution, the Bloch wave includes many periodic units. Figure 2(b) is an enlarged rectangular region in Fig. 2(a). Each unit has six similar parts,

which are repeated after rotating clockwise or counterclockwise by an integral multiple of $2\pi/3$. All these parts can be covered by a circle with a radius r_c, and the field at the boundary of the circle is almost zero. The diameter $2r_c$ is about $1.80a$. It is found that the field distribution in a unit is very close to the amplitude distribution of an oscillation mode on the 2D circular membrane [17]. In Section 3, according to the above investigation, we use the oscillation model of the circular membrane to approximately represent the field distribution in a circular unit of the Bloch wave. Then we obtain the effective refractive indices at normal incidence from its phase velocity. Finally, these results are compared with those calculated by EFSs.

3. OSCILLATION MODEL OF THE CIRCULAR MEMBRANE

A. Wave Solution Of the Circular Membrane

In this section, we deduce the effective refractive index from the modes of the 2D circular membrane. The wave Ψ distributing on the 2D circular membrane satisfies the following equation [18,19]:

$$\left(\frac{\partial^2}{\partial r^2} + \frac{1}{r}\frac{\partial}{\partial r} + \frac{1}{r^2}\frac{\partial^2}{\partial \phi^2}\right)\Psi = \frac{1}{v_c^2}\frac{\partial^2}{\partial t^2}\Psi, \tag{1}$$

where r is the radius and ϕ is the polar angle in the polar coordinate, and v_c is the radial velocity. The wave satisfies the boundary condition $\Psi(r_c, \phi, t) = 0$. Using the separate variable method, the wave can be expanded as the product of three independent functions; that is, $\Psi(r, \phi, t) = R(r)\Phi(\phi)T(t)$. Then Eq. (1) can be further divided into three independent equations:

$$\frac{T''}{v_c^2 T} = -\alpha_{mn}^2, \tag{2}$$

$$-\frac{\Phi''}{\Phi} = m^2, \tag{3}$$

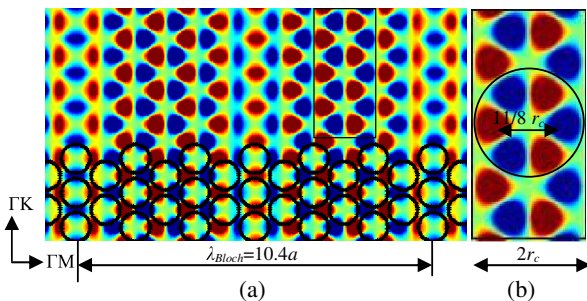$$r^2 R'' + rR' + (\alpha_{mn}^2 r^2 - m^2)R = 0, \tag{4}$$

Fig. 2. (Color online) (a) E_z-field distribution of the TM-polarization Bloch wave with frequency $0.36(c/a)$ in a 2D triangular PhC. Some air holes are denoted as black circles; (b) Field distribution of the rectangular region in (a). Each unit can be covered by a circle.

where both m and n are sets of the nonnegative integer, and α_{mn} is a positive value. Equation (4) is the mth-order Bessel differential equation. If $x = \alpha_{mn}r$ is substituted into Eq. (4), the solution of $R(r)$ is the first kind mth-order Bessel function $J_m(x)$. Considering the boundary condition $J_m(\alpha_{mn}r_c) = 0$, then we have $\alpha_{mn}r_c = K_{mn}$, where K_{mn} is the nth zero ($n = 1, 2, 3\ldots$) of the Bessel function $J_m(x)$. The general time-independent solution of the wave satisfying boundary condition $\Psi(r_c, \phi) = 0$ is

$$\Psi(r, \phi) = \sum_{m=0}^{\infty} \sum_{n=1}^{\infty} J_m\left(\frac{k_{mn}r}{r_c}\right)[p_{mn}\cos(m\phi) + q_{mn}\sin(m\phi)]_. \tag{5}$$

where p_{mn} and q_{mn} are the corresponding coefficients, respectively.

B. Effective Refractive Index In The Negative Refraction Region

After observing the field distribution at $0.36(c/a)$ in Fig. 2, it is found that the field distribution is much like the amplitude distribution in the circular membrane. Since the wave equations of the circular membrane and the PhC are the same except for the propagating velocity on the right-hand side of Eq. (1), we replace the field distribution of the PhC with the amplitude distribution of the circular membrane, that is, the Bessel function J_3. So the phase velocity of the circular membrane is transferred into the phase velocity of the PhC at the same time.

The closest solution of the wave Ψ to our case is the mode of $m = 3$ and $n = 1$. The first zero root of the Bessel function J_3 is $K_{31} = 6.3802$. From Eq. (2), the solution of the time function is $T(t) = A\cos(\alpha_{31}v_c t + \delta)$, where A and δ are the amplitude and phase constant determined by the initial condition, respectively. The $\alpha_{31}v_c$ represents the angular frequency ω_c; that is,

$$\alpha_{31}v_c = K_{31}v_c/r_c = \omega_r = 2\pi f_c, \tag{6}$$

where f_c is the oscillation frequency of the circular membrane. Then the phase velocity v_p is

$$v_p = f_c 2\pi r_c/K_{31}, \tag{7}$$

By replacing the wave function Ψ with the E_z-field, one thing that should be noticed is that Eq. (7) is also the phase velocity of the Bloch wave in the PhC because the E_z-field distribution inside the circular unit is a part of the Bloch wave. The phase velocity v_p is defined by $v_p = c/|n|$, where n is the effective refractive index. When v_p is known, the effective refractive index can be determined simultaneously. From Fig. 2(b), we have obtained $r_c = 0.90a$. The only unknown parameter is f_c. It is the frequency of the circular oscillating membrane and can be found from Figs. 2(a) and 2(b). In a range of λ_{Bloch}, there are about $\lambda_{\text{Bloch}}/2r_c = 5.9$ units. Besides, the horizontal distance of two repeated field distributions in a circular unit is about $11/16$ times the diameter as shown in Fig. 2(b), so the wavelength on the circular membrane is approximated as this distance. Finally, the oscillation frequency f_c approximates to 5.9 times the frequency of the Bloch wave, then multiplies by $16/11$, which results in the value of $3.09(c/a)$. Substituting f_c

into Eq. (7), and using the relation between v_p and n, the effective refractive index of the PhC at this frequency is

$$|n| = 11K_{31}a/16\pi\bar{f}\lambda_{\text{Bloch}}, \tag{8}$$

where $\bar{f}c/a$ is the frequency of the incident light. The wavelengths of Bloch waves from 0.345 to $0.365(c/a)$ are shown in Fig. 3. Each wavelength is determined by the FDTD calculation as the Bloch wavelength is obtained in Fig. 2(a). After fitting the curve of the Bloch wavelength, an approximate relation between the frequency and the Bloch wavelength is

$$\lambda_{\text{Bloch}} = Aa/(\bar{f}_{\text{edge}} - \bar{f}), \tag{9}$$

where $\bar{f}_{\text{edge}} = 0.37$ is the top edge frequency of the second band, and $A = 0.3238$ is a fitting constant. This relation is reasonable and ensures that the definition of λ_{Bloch} is meaningless in the photonic band gap between the second and third photonic bands as shown in Fig. 1(a). The curve fitting of Eq. (9) is also shown in Fig. 3. Substituting Eq. (9) into Eq. (8), the effective refractive index can be related to the wave frequency and the band edge frequency only. It is

$$|n| = 11K_{31}(\bar{f}_{\text{edge}} - \bar{f})/16\pi A\bar{f}. \tag{10}$$

In Eq. (10), the effective refractive index has no definition when the frequency is higher than $\bar{f}_{\text{edge}}$. In order to check the accuracy of this oscillation model, the effective refractive indices calculated by using Eq. (8), Eq. (10), and EFS are all shown in Fig. 4(a). When $\bar{f} = 0.36$ and $\lambda_{\text{Bloch}} = 10.4a$, both Eq. (8) and Eq. (10) obtain $|n| = 0.373$, which is close to the value calculated from EFS, which is $|n| = 0.350$. It also shows that Eqs. (8) and (10) match each other after $0.355(c/a)$, so Eq. (10) can substitute for Eq. (8) near the top of second band very well. In Fig. 3, the Bloch wavelength increases quickly as the frequency increases, but the effective refractive index decreases in its absolute value. Furthermore, the inversely effective refractive indices calculated by EFSs approximately satisfy the Bloch wavelengths multiplied by $\bar{f}/1.311a$. The similarly multiplied factor extracted from Eq. (8) is $\bar{f}/1.396a$. Both multipliers are very close to each other. The oscillation
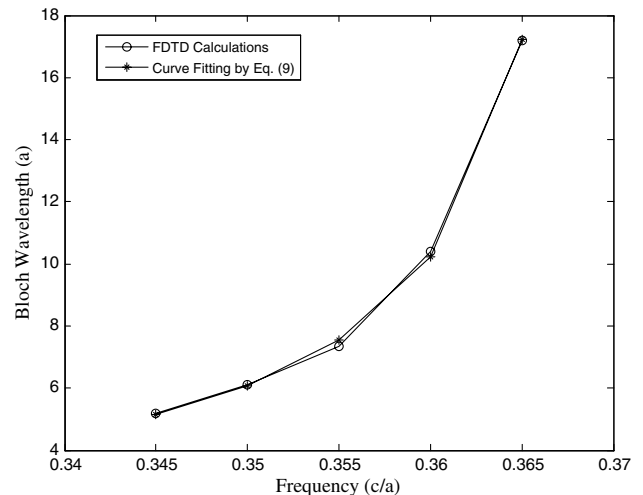

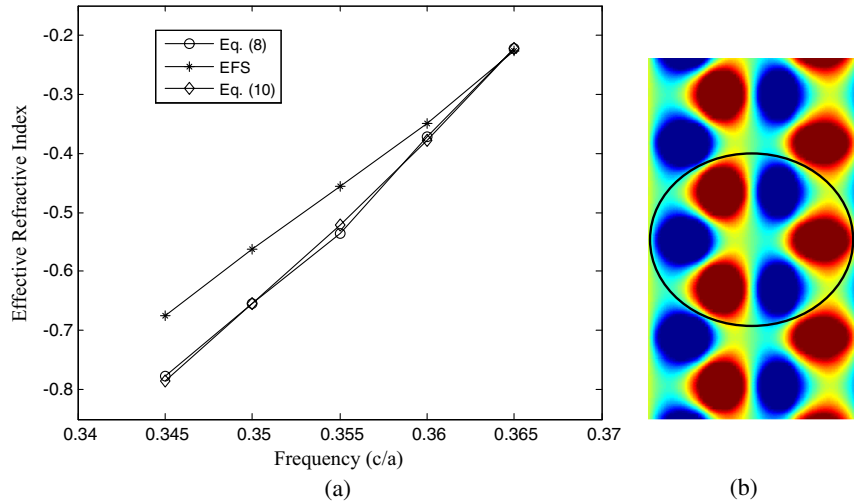Fig. 3.   Wavelengths of the Bloch waves from 0.345 to $0.365(c/a)$ calculated by the FDTD method.

Fig. 4. (Color online) (a) Effective refractive indices from 0.345 to 0.365(c/a) calculated by Eq. (8) and EFSs, respectively. (b) Field distribution in an elliptic unit at 0.345(c/a).

model well deduces the effective refractive index near the top of the second band and gives the field distribution of the circularly repeated unit.

The field distribution in the circular unit is described by the Bessel function J_3 combined with the sine and cosine functions, which is much more concise than the expansion of a lot of Fourier series. However, the difference between EFS and Eq. (8) in Fig. 4(a) becomes explicit as the frequency decreases. It is the reason that the unit of the Bloch wave cannot be covered by a circle perfectly. As a result, the effective refractive indices calculated from EFSs are smaller than those from Eq. (8). An appropriate shape to cover the unit region is an ellipse. A demonstration at 0.345(c/a) is shown in Fig. 4(b), where the unit is lengthened in the ΓM direction.

Our model proposed here shows the relationship between field distributions and effective refractive indices at higher photonic bands. This proposal tries to give another way, which is different from the plane wave expansion (PWE) method and EFSs, to obtain the effective refractive index. We focus on the kind of the circular unit and deduce the equation of the effective refractive index from the Laplace equation in the polar coordinate. Traditionally, the propagation mode in the PhC is given by the PWE method in terms of infinite Fourier series. This model gives another expression in terms of Bessel functions. The cases of noncircular units would be analyzed by the perturbation theory based on the basis of Bessel functions. In general, the corresponding frequency of the circular unit often exists at the photonic band edge as the case near the top of the second photonic bands, so the results give another point of view to discuss the physics or optics near band edges.

Furthermore, the reason this oscillation model can deduce the effective refractive indices close to those calculated from EFSs is that the E_z-field inside the circular unit is like the amplitude on the membrane because both obey the same form of the 2D Laplace equation. Due to the periodicity of the field distribution as shown in Fig. 2, the E_z-field can be solved in a circular unit, which is actually the same as that obtained from the PWE method. In Fig. 2(a), the neighboring fields between two adjacent Bloch wavelength areas and at the middle of each Bloch wavelength area have something different from

the displays shown in Fig. 2(b). It is the fact that the Bloch wavelength at 0.36(c/a) is not an integral multiple of the periodicity of $\sqrt{3}a$ in the ΓM direction. The diameter of each circular unit is 1.80a, which is a little longer than $\sqrt{3}a$. Because a Bloch wavelength range equals to about 5.9 circular units, the field distribution distorts explicitly at phase angles of the neighborhood of 0°, 180°, and 360°. Although it has a little distortion at these phase angles, the field distribution in a circular unit matches that calculated by the PWE method. This means this model as well as the PWE method can be used here.

C. Group Velocity
Finally, the averaged group velocities are calculated by both data in Fig. 4(a). The group velocity in the dispersive medium is [20]

$$v_g = \frac{c}{n + f(dn/df)}, \tag{11}$$

where f is the frequency. For the purpose of the numerical calculation, dn/df is approximated as $\Delta n/\Delta f$, and n and f in Eq. (11) are chosen as the averaged values of two continuous data. The averaged group velocities corresponding to
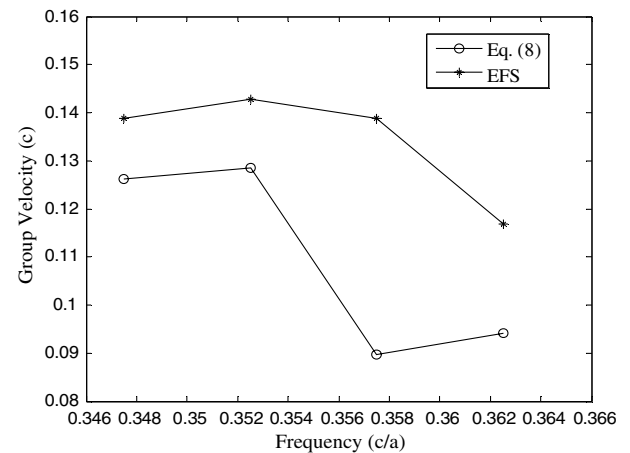

Fig. 5. Group velocities from 0.3475 to 0.3625(c/a) calculated by data in Fig. 4(a).

EFS and Eq. ([8](#)) from 0.3475 to 0.3625(c/a) are shown in Fig. [5](#). The results tell us that both values are close to each other, except for 0.3575(c/a). The averaged velocity in this frequency region is about 0.13c.

4. SUMMARY

In summary, we use the oscillation model of the circular membrane to deduce the effective refractive indices near the top of the second photonic band. It is based on the same Laplace equation in both cases of the membrane and the PhC, and the field in the circular unit of the Bloch wave is approximately equal to the amplitude on the circular membrane. This model not only gives the inverse relation between the Bloch wavelength λ_{Bloch} and the effective refractive index n, but also displays that the effective refractive index can be related to the wave frequency and the band edge frequency. It gives another way to calculate the effective refractive indices of higher photonic bands directly and concisely, and displays the field distributions in terms of the Bessel function, which is more compact than the traditional one by the PWE method. Also largely repeated units of field distributions in PhCs are not like the circular case in this paper; however, it is a good beginning to discuss the relationship between the effective refractive index and the field distribution. Furthermore, the results are applicable to the oblique cases as long as the field distributions have circularly repeated units.

REFERENCES

1. S. John, "Strong localization of photons in certain disordered dielectric superlattices," Phys. Rev. Lett. **58**, 2486–2489 (1987).
2. A. Z. Genack and N. Garcia, "Observation of photon localization in a three-dimensional disordered system," Phys. Rev. Lett. **66**, 2064–2067 (1991).
3. H. Kosaka, T. Kawashima, A. Tomita, M. Notomi, T. Sato, and S. Kawakami, "Superprism phenomena in photonic crystals," Phys. Rev. B **58**, R10096–R10099 (1998).
4. A. L. Pokrovsky and A. L. Efros, "Electrodynamics of metallic photonic crystals and the problem of left-handed materials," Phys. Rev. Lett. **89**, 093901 (2002).
5. M. L. Povinelli, Steven G. Johnson, J. D. Joannopoulos, and J. B. Pendry, "Toward photonic-crystal metamaterials: creating magnetic emitters in photonic crystals," Appl. Phys. Lett. **82**, 1069–1071 (2003).
6. C.-H. Kuo and Z. Ye, "Negative-refraction-like behavior revealed by arrays of dielectric cylinders," Phys. Rev. E **70**, 026608 (2004).
7. D. Felbacq and G. Bouchitté, "Left-handed media and homogenization of photonic crystals," Opt. Lett. **30**, 1189–1191 (2005).
8. A. Martínez and J. Martí, "Negative refraction in two-dimensional photonic crystals: role of lattice orientation and interface termination," Phys. Rev. B **71**, 235115 (2005).
9. I. Bulu, H. Caglayan, and E. Ozbay, "Negative refraction and focusing of electromagnetic waves by photonic crystals," J. Phys. Conf. Ser. **36**, 33–40 (2006).
10. T. Decoopman, G. Tayeb, S. Enoch, D. Maystre, and B. Gralak, "Photonic crystal lens from negative refraction and negative index to negative permittivity and permeability," Phys. Rev. Lett. **97**, 073905 (2006).
11. T.-H. Pei and Y.-T. Huang, "Analyzing the propagating waves in the two-dimensional photonic crystal by the decoupled internal-field expansion method," AIP Advances **2**, 012188 (2012).
12. M. Notomi, "Theory of light propagation in strongly modulated photonic crystals: refractionlike behavior in the vicinity of the photonic band gap," Phys. Rev. B **62**, 10696–10705 (2000).
13. T.-H. Pei and Y.-T. Huang, "The high-transmission photonic crystal heterostructure Y-branch waveguide operating at photonic band region," J. Appl. Phys. **109**, 034504 (2011).
14. T.-H. Pei and Y.-T. Huang, "The equivalent structure and some optical properties of the periodic-defect photonic crystal," J. Appl. Phys. **109**, 073014 (2011).
15. T.-H. Pei and Y.-T. Huang, "The heterostructure photonic crystal waveguide splitter," IEEE Photon. Technol. Lett. **23**, 1145–1147 (2011).
16. A. Taflove and S. C. Hagness, *Computational Electrodynamics*, 2nd ed. (Artech House, 2000).
17. G. B. Arfken, H. J. Weber, and F. Harris, *Mathematical Methods for Physicists: A Comprehensive Guide*, 6th ed. (Academic, 2005).
18. M. R. Spiegel and J. Liu, *Mathematical Handbook of Formulas and Tables*, 2nd ed. (McGraw-Hill, 1999).
19. I. S. Gradshteyn and I. M. Ryzhik, *Table of Integrals, Series, and Products*, 7th ed. (Academic, 2007).
20. J. D. Jackson, *Classical Electrodynamics*, 2nd ed. (Wiley, 1990).